NIH Public Access
Author Manuscript
Rev Sci Instrum. Author manuscript; available in PMC 2011 January 11.

Published in final edited form as:
Rev Sci Instrum. 2007 June ; 78(6): 063707. doi:10.1063/1.2745733.

Easy and direct method for calibrating atomic force microscopy lateral force measurements

Wenhua Liu, **Keith Bonin**, and **Martin Guthold**[a)]
Department of Physics, Wake Forest University, Winston-Salem, North Carolina 27109

Abstract

We have designed and tested a new, inexpensive, easy-to-make and easy-to-use calibration standard for atomic force microscopy (AFM) lateral force measurements. This new standard simply consists of a small glass fiber of known dimensions and Young's modulus, which is fixed at one end to a substrate and which can be bent laterally with the AFM tip at the other end. This standard has equal or less error than the commonly used method of using beam mechanics to determine a cantilever's lateral force constant. It is transferable, thus providing a universal tool for comparing the calibrations of different instruments. It does not require knowledge of the cantilever dimensions and composition or its tip height. This standard also allows direct conversion of the photodiode signal to force and, thus, circumvents the requirement for a sensor response (sensitivity) measurement.

INTRODUCTION

The atomic force microscope (AFM) is not only a good tool in imaging sample topography at high resolution, but it is also frequently used in probing the mechanical properties of materials on the nanometer scale. For example, AFMs have been used to study the compliance, stiffness, adhesion, and frictional properties of biological and nonbiological samples.[1–3] AFM force measurements may be divided into normal force and lateral force measurements. In normal force measurements, the cantilever is moved normally to the surface. This method has been used in compliance measurements of cells,[4] in single-protein unfolding,[3] and single-molecule stretching experiments.[5] In lateral force measurements, the cantilever is moved parallel to the surface. This method has been used in friction measurements or to stretch fibers. For example, the nanoscopic, frictional forces between functionalized tips and surfaces have been determined[2,6] and the mechanical properties of viruses, DNA, carbon nanotubes, and fibrin fibers have been measured.[7–9]

In all AFM force measurements, the AFM cantilever is used to apply forces to the sample under investigation. To extract reliable, quantitative values for material properties from these measurements, the applied forces need to be accurately known, which, in turn, critically depends on reliable and universally applicable force calibration methods for AFM instruments. As outlined below, several calibration methods, each with its own advantages and disadvantages, have been described to date. To better understand some lateral force calibration methods, normal force calibration methods will also need to be discussed peripherally.

Typically, in an AFM, a laser beam is focused on the back of the cantilever, which has a mirrored surface that reflects the beam into a four-quadrant photodiode (Fig. 1). An up-

[a)]Author to whom correspondence should be addressed; Tel.: 336-758-4977; Fax: 336-758-6142; electronic mail: gutholdm@wfu.edu.

NIH-PA Author Manuscript
NIH-PA Author Manuscript
NIH-PA Author Manuscript

NIH-PA Author Manuscript

NIH-PA Author Manuscript

NIH-PA Author Manuscript

down deflection of the cantilever x_n caused by a normal force F_n results in a change in the top–bottom photocurrent I_n. A lateral (torsional) deflection of the cantilever x_l, caused by a lateral force F_l, results in a change in the left–right photocurrent I_l. The challenge in all AFM force measurements is to convert the measured signal, photocurrent, to the desired quantity: force.

The lateral force calibration methods that are used for this conversion may generally be divided into the following categories:

- Theoretical methods, in which the cantilever force constant is calculated from beam mechanics using elasticity theory. It requires accurate knowledge of the dimensions and moduli of the cantilever.
- Dynamic methods, in which the cantilever force constant is obtained by analyzing the resonance frequency of cantilevers. These methods may be combined with the theoretical method to yield better results.[10]
- The wedge method, in which both normal and lateral force responses of the cantilever are examined during friction measurements on sloped surfaces.
- Methods in which a known force is applied to the cantilever via artifacts or external means. Our method is of this type.

Theoretical and dynamic methods

Perhaps the quickest and most commonly used calibration method is using beam mechanics (elasticity theory) to calculate the normal and lateral force constants of a cantilever.[10–12] When performing normal force measurements, the tip is deflected by an amount x_n normal to the surface, either by pushing down on the surface or by pulling on a molecule that is anchored between the tip and the surface. The applied force may be calculated from Hooke's law and beam mechanics as[10–13]

$$F_n = k_n x_n \tag{1a}$$

$$= k_n S_n I_n. \tag{1b}$$

$S_n = x_n/I_n$ is called the normal sensitivity (or sensor response) and it relates the normal displacement x_n and the resulting photocurrent in the photodiode I_n. It is determined by engaging the tip on a hard surface and ramping the surface up and down while measuring the resulting photocurrent. Unfortunately, this procedure can sometimes damage the tip. The spring constant k_n, for bending a cantilever with *rectangular* cross section, fixed on one end is

$$k_n = \frac{Ewt^3}{4l^3}. \tag{2}$$

For other cantilever shapes, k_n will be different and more difficult to calculate.

Thus, for a cantilever with rectangular cross section,

NIH-PA Author Manuscript

NIH-PA Author Manuscript

NIH-PA Author Manuscript

$$F_n = \frac{Ewt^3}{4l^3} S_n I_n. \tag{3}$$

Equation (3) relates the desired quantity F_n to the measured quantity I_n. E is the Young's modulus, w is the width, t is the equivalent thickness, and l is the length of the cantilever (Fig. 1). To account for the tip in the other end, an equivalent thickness t, instead of the real thickness, is often calculated from the cantilever resonance frequency f via the following equations:

$$f = \frac{1}{2\pi} \sqrt{\frac{Ewt^3}{4l^3(m_t + 0.236m_c)}} \tag{4a}$$

$$= 0.276 \sqrt{\frac{Ewt^3}{\rho(\pi h^3 l^3 + 0.2832wtl^4)}}. \tag{4b}$$

Here, ρ is the density of the cantilever material; m_t and m_c are the masses of the tip and cantilever.

In lateral force measurements, the tip is moved laterally (parallel to the surface) and the apex of the tip is deflected sideways by an amount x_l. In this case, the applied force is given by Hooke's law as

$$F_l = k_l x_l \tag{5a}$$

$$= k_l S_l I_l \tag{5b}$$

$$= K_C I_l. \tag{5c}$$

The goal in all lateral force calibration methods is to determine K_C, which we will call the *lateral force conversion factor*. It relates the measured photocurrent I_l to the desired applied lateral force F_l. For a cantilever with rectangular cross section, the lateral force constant is

$$k_l = \frac{Gwt^3}{3l(h + t/2)^2}. \tag{6}$$

Here, G is the shear modulus of the cantilever and h is the height of the tip.

Thus, combining Eqs. (5c) and (6), for such a cantilever,

NIH-PA Author Manuscript

NIH-PA Author Manuscript

NIH-PA Author Manuscript

$$F_l = \frac{Gwt^3}{3l(h+t/2)^2} S_l I_l. \tag{7}$$

Here, I_l is the left–right photocurrent and $S_l = x_l/I_l$ is the lateral sensitivity of the microscope. The lateral sensitivity (photodiode response) may be determined by direct, experimental measurement from the "stick" slope in a friction loop.[14]

S_l may also be determined through the normal sensitivity S_n via

$$S_l = \frac{E(h+t/2)}{2Gl} S_n. \tag{8}$$

However, here it is assumed that the photodiode is "rotationally symmetric;" that is, a certain displacement φ of the laser beam in the up-down or the left-right direction will result in the same photocurrent. This is often not exactly the case (due to diffraction effects from the cantilever as well as the possible asymmetry of diode laser divergence angles) and may induce errors. The factor $E(h+t/2)/2Gl$ comes from the fact that the same deflection in the normal or lateral direction of a bent cantilever, x_n and x_l, results in different *angular* cantilever deflections, θ_n and θ_l. θ_n and θ_l are related by $\theta_l = [E(h+t/2)/2Gl]\theta_n$.

Thus, using Eqs. (7) and (8), for a cantilever with rectangular cross section

$$F_l = \frac{Ewt^3}{6l^2(h+t/2)} S_n I_l \tag{9}$$

and, comparing with Eq. (5c), the desired lateral force conversion factor K_C for such a cantilever can be calculated via

$$K_C = \frac{Ewt^3}{6l^2(h+t/2)} S_n. \tag{10}$$

We will compare the K_C calculated from this equation (based on cantilever beam mechanics) with the one obtained from our glass fiber method.

The cantilever beam mechanics method [Eq. (10)] requires accurate knowledge of the cantilever's elastic moduli and dimensions. Hence, it works best for simple diving board cantilevers with rectangular cross sections and uniform thickness. It is more difficult to apply this to cantilevers with irregular shapes, to bilayer levers, such as gold coated silicon nitride levers, or to heavily modified cantilevers. Moreover, lever thickness and tip height are sometimes difficult to determine accurately. Finite element analysis may be used for calculating the spring constants of more complex levers.[15] However, finite element analysis still requires accurate knowledge of the cantilever dimensions.

Cleveland *et al.* developed a dynamic method to calculate the normal spring constant of an AFM cantilever.[16] In this method, small spheres (or gold coating[17]) of known mass are attached to the cantilever. By monitoring the resulting change in the cantilever's resonant

NIH-PA Author Manuscript

NIH-PA Author Manuscript

NIH-PA Author Manuscript

frequency, the spring constant of the cantilever can be determined. This method has the disadvantage that each cantilever needs to be handled and modified with a sphere, which increases the chance for breaking the cantilever or altering its properties. Also, the location of the sphere on the cantilever and the sphere's mass need to be known accurately. The dynamic method may also be used to determine lateral force constants.[12] However, the resonance frequencies for torsional oscillations are often too high to be detected by standard AFM equipment; thus, this method usually requires special, external oscilloscopes.

The equipartition theorem, $k_B T = \frac{1}{2} k_n \Delta x_n^2$, has been used to obtain the normal force constant[18] by measuring the thermal fluctuations of the cantilever Δx^2. This is an elegant method for obtaining the cantilever force constants that is actually included in some microscope software packages. However, it works less well for stiffer cantilevers and for lateral force calibration, because the thermal fluctuations Δx^2 become small as compared to other noise. Moreover, when using this method for lateral force calibrations, the height of the tip is needed, since only the *torsional* spring constant can be determined.

Wedge method

Ogletree *et al.* developed the wedge calibration method to experimentally determine the lateral force response of a cantilever.[19] It is based on comparing the lateral force signals and normal force signals on surfaces with known slopes. Assuming that the width of the wedge is significantly larger than the tip radius (which is almost always the case), this method does not require knowledge of the shape of the tip. Only higher order corrections, which rely on a contact mechanics model (e.g., Hertz model), would require knowledge of the shape of the tip. Recently, Asay and Kim[20] described a method that utilizes a careful analysis of force curves taken on substrates with known slopes to extract the lateral and normal force responses of cantilevers.

Applied force methods

Different artifacts or applied external forces have also been used to calibrate AFM lateral force measurements. Bogdanovic *et al.*[21] used a tiny, very sharp spike (an upside down AFM tip) as a device to determine the lateral spring constant of a tipless cantilever. The cantilever is pushed down on the tiny sharp spike at an offset, which results in a normal and lateral deflection of the cantilever. It is a feasible though complex and experimentally difficult method. Feiler *et al.*[22] attached a small glass fiber, that functions as a lever, directly to the cantilever. In their method, the vertical and lateral deflections of the cantilever, due to the force on the attached lever, are measured simultaneously. This method has the disadvantage that the cantilever needs to be modified with a relatively large glass fiber that may interfere with subsequent measurements. Morel *et al.*[23] used a cantilevered glass fiber to calibrate AFM normal and lateral force measurements. Their setup is somewhat similar to ours. However, they used a much larger and stiffer fiber, so the lateral force calibration had to be determined via a friction loop taken on top of the suspended glass fiber, which complicates the analysis. Their analysis relies on a clearly discernible separation of the force to deflect the glass fiber and the frictional force in the obtained force traces. If the frictional force is smaller than the force to significantly deflect the glass fiber, the method may fail. Cumpson *et al.*[24] developed a microelectromechanical system (MEMS) device called lateral electrical nanobalance (LEN) for calibrating lateral force measurements in an AFM. This is an accurate though labor- and cost-expensive and technically complex method. Recently, Li *et al.* developed a diamagnetic levitation spring system to calibrate AFM lateral force measurements.[25] In this system, a levitated, diamagnetic sheet is used to apply known forces to the AFM tip. Jeon *et al.*[26] coated a cantilever with gold which then could be twisted by inducing a Lorentz current via an external magnetic field.

NIH-PA Author Manuscript

NIH-PA Author Manuscript

NIH-PA Author Manuscript

In many of these methods the setup or analysis is technically complex.[20–26] Others[10–12,15–17] only determine the lateral force constant of the cantilever k_l, and, thus, accurate conversion of the measured photocurrent into force still requires an accurate determination of the sensitivity S_l [Eq. (5b)] and tip height [Eq. (8)]. The wedge methods[19] require special substrates with known slopes. Some methods also require accurate knowledge of the normal force constant.[19,20]

Here, we present an alternative experimental procedure for calibrating AFM lateral force measurements that is inexpensive, easy to make, and easy to use. This method may be used to calibrate any cantilever, regardless of its size, stiffness, shape, material, or coating. Moreover, this method does not require sensitivity measurements of the cantilever, since the photodiode signal is directly converted to force. It is transferable and may thus be used as a universal calibration standard. Our calibration method consists of a small glass fiber of known dimensions (about 100 μm in length, 1 μm in diameter) and Young's modulus, which is glued down at one end to a substrate and which can be bent laterally with the AFM tip at the other end.

We have utilized a combined AFM/optical microscope to record movies of the bent glass fiber via optical microscopy, assuring that our method works as envisioned.

We are also quantitatively comparing our method with the theoretical method based on beam mechanics [Eq. (10)].

MATERIALS AND METHODS

Preparation of Glass fiber sample

A bundle of glass fibers (Johns-Manville Corp, Denver, Colorado) was deposited onto a clean, glass slide (Fisher Scientific, Pittsburgh, PA). A single fiber was extracted from the cluster with superfine tweezers and glued at one end to a glass slide with a drop of nail polish (about 0.5 μl, Sally Hansen; Uniondale, NY). The whole process was performed under a stereo microscope (Leica Zoom 2000, Fisher, Pittsburgh, PA) with adjustable zoom. Since the lateral force generated by AFM cantilevers is on the order of nanonewtons, the ideal size of the glass fiber is about 100 μm in length and 1 μm in radius [see Eq. (11)]. The orientation of this glass fiber is parallel to the AFM cantilever. The radius of the fiber can be determined with an error of less than 3% by AFM or scanning electron microscopy (SEM). It is difficult to accurately determine the radius by optical microscopy, because of the fringes created by diffraction and refraction at the edge of the glass fiber.

Glass fiber bending experiments

The glass fiber sample was placed in our combined atomic force/optical microscope instrument. The instrumentation setup and schematics are shown in Fig. 2. Optical microscopy was performed with an inverted Zeiss Axiovert 200 microscope (Zeiss, Göttingen, Germany), a Hamamatsu EM-CCD C9100 Camera (Hamamatsu Photonics KK, Japan), and IPLAB software (Scanalytics, Fairfax, VA). The atomic force microscope (Topometrix Explorer, Veeco Instruments, Woodbury, NY) fits on the stage of the optical microscope.[9,27] The stage can be moved so that the AFM tip is aligned with the objective lens of the optical microscope. Additionally, once the AFM and the objective lens are aligned, the sample can be moved independently of both microscopes via *x*-*y*-*z* micrometer screws. With this instrument it is possible to take AFM and optical images simultaneously or alternatively take optical images (movies) of an object that is manipulated by the AFM. The Topometrix Explorer has an open loop piezo which increases the error in position measurements.

NIH-PA Author Manuscript

NIH-PA Author Manuscript

NIH-PA Author Manuscript

The AFM manipulation experiments were done with a NANOMANIPULATOR (3rd Tech, Chapel Hill, North Carolina), which is a software program that interfaces the AFM with a force feedback stylus (PHANTOM, Sensable Technologies, Woburn, MA) and a graphics computer.[7] The NANOMANIPULATOR provides control over the motion of the AFM tip in the *x*, *y*, and *z* directions. For these experiments, the AFM tip was pushed down normally on the surface with a small, constant normal force and moved laterally in a user-defined path.

AFM Cantilevers

We used three different types of cantilevers with rectangular cross sections and which had a range of normal force constants from 0.053 to 1.38 N/m (see Table I): NCL-W (Nanosensors, Neuchatel Switzerland), NT-MDT CSCS12, and NSC12 silicon cantilevers (Silicon-MDT Ltd., Moscow, Russia). The dimensions for each type of cantilever are provided by the manufacturer; however, since there are variations, we determined the cantilever length, width, and tip height via optical microscopy (40× or 100× objective lens). The resonance frequencies of the cantilevers and sensor response were obtained via standard AFM operating procedures. Using beam mechanics, the normal and lateral force constants were calculated from these data via Eqs. (2) and (6). Also listed in Table I is the "lateral force conversion factor" K_C for converting photocurrent (units: ampere) into force (units: newton), as calculated from Eq. (10) and via our glass fiber method. K_C is listed because it is the critical lateral force conversion factor that is needed in all calibration methods and that is obtained *directly* via our calibration method.

RESULTS AND DISCUSSION

Figure 3 shows an optical, AFM, and SEM image of a representative glass fiber. The radius of the glass fiber can be accurately determined via AFM and SEM. Frames from a movie sequence of a glass fiber manipulation are shown in Fig. 4 (for movie see Ref. [28]). The dark rectangle is the AFM cantilever as seen from underneath by optical microscopy. The glass fiber is first bent forward by the AFM tip and it then returns elastically to its straight position as the AFM tip moves back. The direction of the cantilever movement is perpendicular to the axis of the glass rod. The tip appears to be leading the fiber, rather than pushing; this is due to optical parallax, as the AFM cantilever is not in the same focal plane as the glass fiber. In the movie, it can be seen more clearly that the tip is indeed pushing the glass fiber. During these experiments, force traces like the one shown in Fig. 4(e) are recorded. These force traces are used to *directly* convert the left–right photocurrent into the applied sample force, i.e., to obtain the lateral force conversion factor K_C. Plotted on the *y* axis is the left–right signal of the photodiode (lateral force signal); the units are nanoampere (nA). Plotted on the bottom *x* axis is the deflection Δy of the glass fiber (as determined from AFM). For small deflections of the glass rod Δy ($\Delta y \ll L$), the bending force F is proportional to the deflection of the glass rod,[13]

$$F = \frac{3E_g \pi r^4}{4L^3} \Delta y. \tag{11}$$

Here, E_g, r, and L are the Young's modulus, radius, and length of the glass fiber. Thus, using this equation, the force can be plotted on the top *x* axis, and the slope of the graph in Fig. 4(e) is $1/K_C$.

For the fiber in Fig. 4(e), E_g =68 GPa, r =1.06 μm, and L=78 μm. The red circles correspond to the forward motion and the blue dots correspond to the backward motion. The slight

NIH-PA Author Manuscript

NIH-PA Author Manuscript

NIH-PA Author Manuscript

difference between the forward (higher force) and backward traces is most likely caused by frictional forces between the tip and the substrate and the fiber and the substrate. In figure 4E, the magnitude of those frictional forces is on the order of 0.5 nA (~20 nN; see K_C =41.1 N/A below). This force is small, but not negligible, as compared to the force to bend the fiber. Since the frictional force is opposite to the direction of motion, it increases the force during forward motion and it decreases the force during backward motion. We reason that averaging the forward and backward curves eliminates the frictional force, yielding the black line in Fig. 4(e). The slope of this line is 2.43×10^{-2} A/N and thus the lateral force conversion factor K_C =41.1 N/A for this particular cantilever and setup.

It should be noted that, for larger deflections (Δy approaching L), the force deviates significantly from linearity and frictional effects may increase [Fig. 4(f)]. The nonlinearity in Fig. 4(f) could also be caused by using a microscope with an open loop piezo. Thus, when using our calibration method, care should be taken that Δy is much smaller than L. This is easily doable, though, as shown in Fig. 4(e). Care should also be taken to account for the frictional forces mentioned above; averaging the forward and backward motion should eliminate most frictional forces. Additionally, it may be possible to reduce frictional forces by slightly angling the glass rod off the surface or by using lubricants.

Each cantilever was used to bend the glass rod at different lengths L. For each value of L, the lateral force conversion factor K_C was calculated as outlined above in Fig. 4(e). Figures 5(a)–5(c) show a plot of the conversion factor K_C vs L (red diamonds). Also plotted in Figs. 5(a)–5(c) (solid blue line) is K_C as calculated from beam mechanics via Eq. (10).

Both methods inevitably have some error sources. Our glass fiber calibration method requires knowledge of r, L, Δy, and E_g [Eq. (11)]. The quantities r and L can be determined with good accuracy via AFM or SEM images, and the deflection Δy can be measured accurately with the AFM (best accuracy is obtained with closed loop piezoes). The Young's modulus of glass is well known. The error in these measurements is on the order of: 3% in r, 3% in L, and 5% in Δy, resulting in an overall error in K_C of about 26%. This uncertainty is displayed as error bars in Figs. 5(a)–5(c). The error for the beam mechanics method can be estimated from the uncertainties of the quantities in Eq. (10): l, 2%; w, 2%; t, 10%; h, 10%; and S_n, 10%, yielding an overall error in K_C of about 56%. Moreover, this calculation implicitly assumes that the lateral sensitivity and normal sensitivity of the photodiode are the same, which may or may not be true (the AFM manufacturer did not divulge these details).

Ideally, in Figs. 5(a)–5(c), the lateral force conversion factor K_C should be a constant value for the same tip and same alignment conditions; though a slight increase with increasing L may be seen in all three graphs. These variations likely stem from the assumption $L \gg \Delta y$, which was made in deriving Eq. (11). For increasing Δy, the contact point of the AFM tip with the glass fiber will migrate a small distance along the fiber axis, thus resulting in a smaller spring constant because of the increasing value of L [see Eq. (11)]. Thus, the lateral force conversion factor obtained for larger L ($\Delta y \ll L$ is better satisfied) should be the more accurate one. Nevertheless, for each individual tip, the lateral force conversion factor K_C determined at various lengths L shows very consistent results, with small standard deviations of 6.4%, 11.3%, and 9.4% for tips 1, 2, and 3, respectively. Figure 5(d) shows a comparison of K_C as determined by both methods. Here the error bars correspond to the standard deviation. Although the fiber appears firmly anchored [in Figs. 4(a)–4(d)], we cannot rule out the possibility that the glue-fiber junction may not be totally rigid or that the glue is slightly compliant. This may also induce small, additional errors and may account for the trend of K_C slightly increasing with L.

NIH-PA Author Manuscript

NIH-PA Author Manuscript

NIH-PA Author Manuscript

As mentioned, the cantilever beam mechanics method will yield the best results when the cantilevers have a simple geometry, uniform thickness, and no coating. In our experiments, we intentionally picked all rectangular cantilevers with no coating on them, so that the data could be easily compared with our glass fiber method. For those cantilevers, the two methods actually yield similar results and errors of similar magnitude. However, as the geometry and material composition of the cantilevers become complicated, the uncertainty of the beam mechanics method will increase significantly. Moreover, the sensor response measurement also affects the accuracy of this method and it can sometimes damage the AFM tips.

Accurate calibration of AFM cantilevers is critical for obtaining reliable values for the mechanical properties of the studied materials. We have introduced a new, inexpensive, easy-to-use, and easy-to-make technique to calibrate AFM lateral force measurements. Our method shows similar uncertainties as the traditional method, based on cantilever beam mechanics, when using simple cantilever geometries. However, our method should be better when using more complex or coated cantilevers. In fact, our calibration method may be applied to any cantilever, made of any material. At the very least, our method can be used to verify the results of other calibration methods. Our nondestructive calibration method is a transferable, universal calibration standard, independent of sensor response measurements and, thus, constitutes a general lateral force calibration standard. The combined inverted optical and atomic force microscope setup is very useful; however, our method could also be used with just the AFM. In this case, the length of the tip needs to be predetermined. The length L for each calibration push can then be determined from AFM scans.

Supplementary Material

Refer to Web version on PubMed Central for supplementary material.

Acknowledgments

The authors would like to thank Anita McCauley for her assistance with obtaining the electron microscopy images. They would like to thank George Holzwarth for help with the glass fiber sample preparation. This work was supported by grants from the Research Corporation (RI0826), the American Cancer Society (IRG-93-035-6), the National Cancer Institute (1 R41 CA10312-01), Wake Forest University (WFU) start-up funds, a WFU Science Research Fund, and a WFU Cross-Campus grant.

References

1. Heinzelmann H, Meyer E, Brodbeck D, Overney G, Guntherodt HJ. Z Phys B: Condens Matter 1992;88(3):321.Frisbie CD, Rozsnyai LF, Noy A, Wrighton MS, Lieber CM. Science 1994;265:2071. [PubMed: 17811409] Grandbois M, Beyer M, Rief M, Clausen-Schaumann H, Gaub HE. 1999;283:1727. ibid. Tomanek, D. Scanning Tunneling Microscopy. Wiesendanger, R.; Guntherodt, H-J., editors. Vol. 3. Springer; Berlin: 1993. p. 269Clausen-Schaumann H, Seitz M, Krautbauer R, Gaub HE. Curr Opin Chem Biol 2000;4(5):524. [PubMed: 11006539]
2. Overney R, Meyer E. MRS Bull 1993;18(5):26.
3. Rief M, Gautel M, Oesterhelt F, Fernandez JM, Gaub HE. Science 1997;276:1109. [PubMed: 9148804]
4. A-Hassan E, Heinz WF, Antonik MD, D'Costa NP, Nageswaran S, Schoenenberger CA, Hoh JH. Biophys J 1998;74(3):1564. [PubMed: 9512052] Hoh JH, Schoenenberger CA. J Cell Sci 1994;107:1105. [PubMed: 7929621]
5. Marszalek PE, Oberhauser AF, Pang YP, Fernandez JM. Nature (London) 1998;396:661. [PubMed: 9872313]
6. Israelachvili, JN. Fundamentals of Friction: Macroscopic and Microscopic Processes. Singer, IL.; Pollock, HM., editors. Kluwer; Dordrecht: 1992. p. 351

NIH-PA Author Manuscript

NIH-PA Author Manuscript

NIH-PA Author Manuscript

7. Guthold M, Falvo MR, Matthews WG, Paulson S, Washburn S, Erie D, Superfine R, Brooks FP, Taylor RM. IEEE/ASME Trans Mechatron 2000;5:189.
8. Wong EW, Sheehan PE, Lieber CM. Science 1997;277:1971.Liu W, Jawerth LM, Sparks EA, Falvo MR, Hantgan RR, Superfine R, Lord ST, Guthold M. 2006;313:634. ibid. Falvo MR, Washburn S, Superfine R, Finch M, Brooks FP, Chi V, Taylor RM. Biophys J 1997;72:1396. [PubMed: 9138585] Falvo MR, Clary GJ, Taylor RM, Chi V, Brooks FP, Washburn S, Superfine R. Nature (London) 1997;389:582. [PubMed: 9335495]
9. Guthold M, Liu W, Stephens B, Lord ST, Hantgan RR, Erie DA, Taylor RM, Superfine R. Biophys J 2004;87:4226. [PubMed: 15465869]
10. Sader JE, Larson I, Mulvaney P, White LR. Rev Sci Instrum 1995;66:3789.
11. Neumeister JM, Ducker WA. Rev Sci Instrum 1994;65:2527.
12. Green CP, Lioe H, Cleveland JP, Proksch R, Mulvaney P, Sader JE. Rev Sci Instrum 2004;75:1988.
13. Young, WC.; Budynas, RG. Roark's Formulas for Stress and Strain. 7. McGraw-Hill; New York: 2002.
14. Carpick RW, Ogletree DF, Salmeron M. Appl Phys Lett 1997;70:1548.Lantz MA, O'Shear SJ, Welland ME, Johnson KL. Phys Rev B 1997;55:10776.
15. Hazel JL, Tsukruk VV. Trans ASME, J Tribol 1998;120(4):814.
16. Cleveland JP, Manne S, Bocek D, Hansma PK. Rev Sci Instrum 1993;64:403.
17. Gibson CT, Weeks BL, Lee JRI, Abell C, Rayment T. Rev Sci Instrum 2001;72:2340.
18. Hutter JL, Bechhoefer J. Rev Sci Instrum 1993;64:3342.1993;64:1868.
19. Ogletree DF, Carpick RW, Salmeron M. Rev Sci Instrum 1996;67:3298.Varenberg M, Etsion I, Halperin G. 2003;74:3362. ibid. Tocha E, Schonherr H, Vancso GJ. Langmuir 2006;22:2340. [PubMed: 16489827]
20. Asay DB, Kim SH. Rev Sci Instrum 2006;77:043903.
21. Bogdanovic G, Meurk A, Rutland MW. Colloids Surf, B 2000;19(4):397.
22. Feiler A, Attard P, Larson I. Rev Sci Instrum 2000;71:2746.
23. Morel N, Ramonda M, Tordjeman P. Appl Phys Lett 2005;86:163103.
24. Cumpson PJ, Hedley J, Clifford CA. J Vac Sci Technol B 2005;23:1992.
25. Li Q, Kim KS, Rydberg A. Rev Sci Instrum 2006;77:065105.
26. Jeon S, Braiman Y, Thundat T. Appl Phys Lett 2004;84:1795.
27. Stephens, BJ. Honors thesis. Wake Forest University; 2005.
28. See EPAPS Document No. E-RSINAK-78-030706 for the glass fiber bending movie. This document can be reached via a direct link in the online article's HTML reference section or via the EPAPS homepage (http://www.aip.org/pubservs/epaps.html).

NIH-PA Author Manuscript

NIH-PA Author Manuscript

NIH-PA Author Manuscript

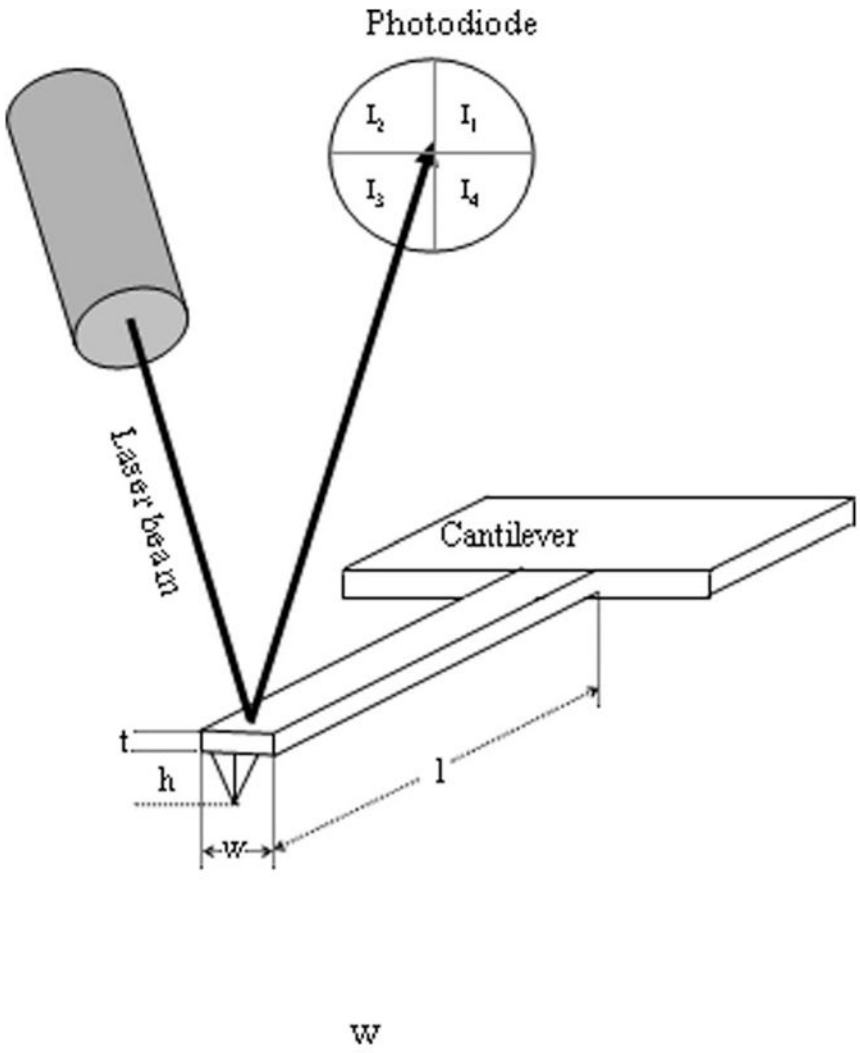

FIG. 1.

Schematic diagram of an AFM with a rectangular cantilever. The position sensitive photodetector contains four photodiodes. Photocurrents I_i collected by these four diodes are used to determine movements of cantilever. A normal force applied to the cantilever will cause a change in the top–bottom signal $I_n \propto [(I_1 + I_2) - (I_3 + I_4)]/\Sigma I_i$; a lateral force will result in a change in the left–right signal $I_l \propto [(I_2 + I_3) - (I_1 + I_4)]/\Sigma I_i$.

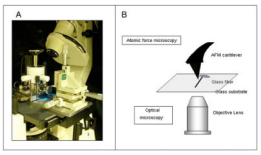

FIG. 2.
(Color online) (A) Photograph and (B) schematics of the experimental setup.

NIH-PA Author Manuscript
NIH-PA Author Manuscript
NIH-PA Author Manuscript

NIH-PA Author Manuscript

NIH-PA Author Manuscript

NIH-PA Author Manuscript

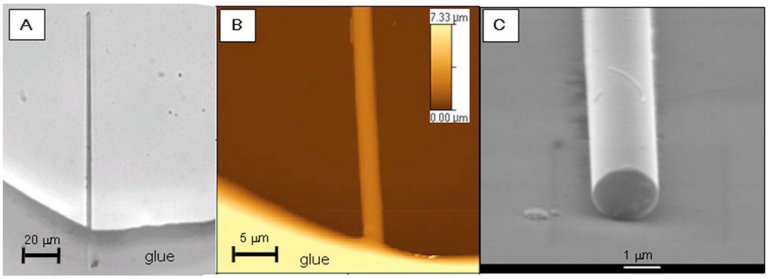

FIG. 3.

(Color online) Images of a glass fiber fixed at one end of the glass substrate. (A) Optical image (top view of the entire fiber), (B) AFM topography image of the fixed end of the glass fiber, and (C) SEM image of the free end of the glass fiber.

NIH-PA Author Manuscript

NIH-PA Author Manuscript

NIH-PA Author Manuscript

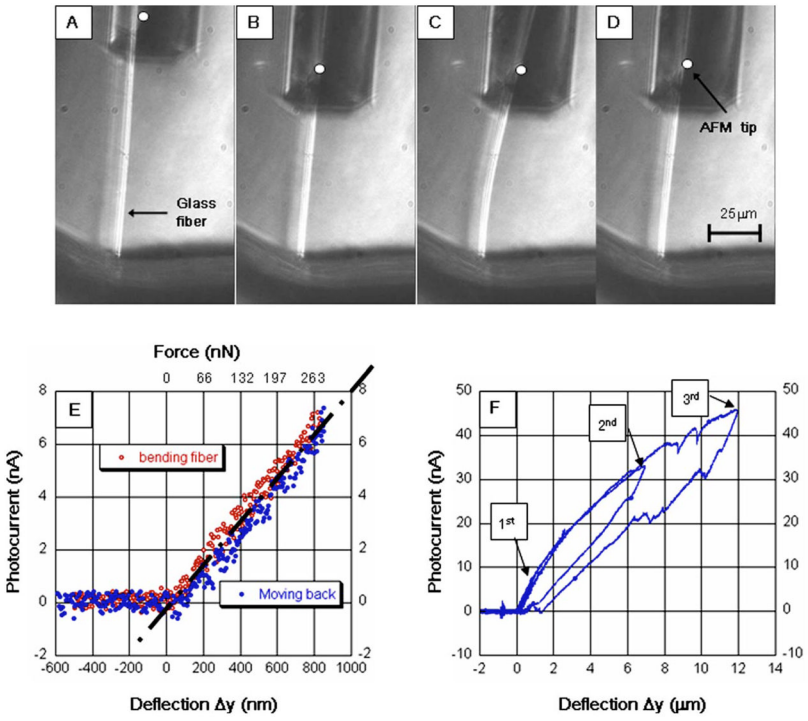

FIG. 4.

(Color online) [(A–D)] Movie frames of a glass fiber that is laterally pushed by the AFM cantilever. (E) A plot of the lateral force (photocurrent) vs the glass fiber deflection, Δy (bottom x axis) and the force to bend the glass fiber (top x axis), calculated via Eq. (11). The red dots correspond to the forward and the blue dots to the backward motion of the cantilever. The black line is the average of both curves. The slope of this curve corresponds to $1/K_C$. (F) As Δy increases (Δy approaches L), the lateral force becomes nonlinear and frictional effects increase (first push: 850 nm; second push: 7 μm; third push: 12 μm).

NIH-PA Author Manuscript

NIH-PA Author Manuscript

NIH-PA Author Manuscript

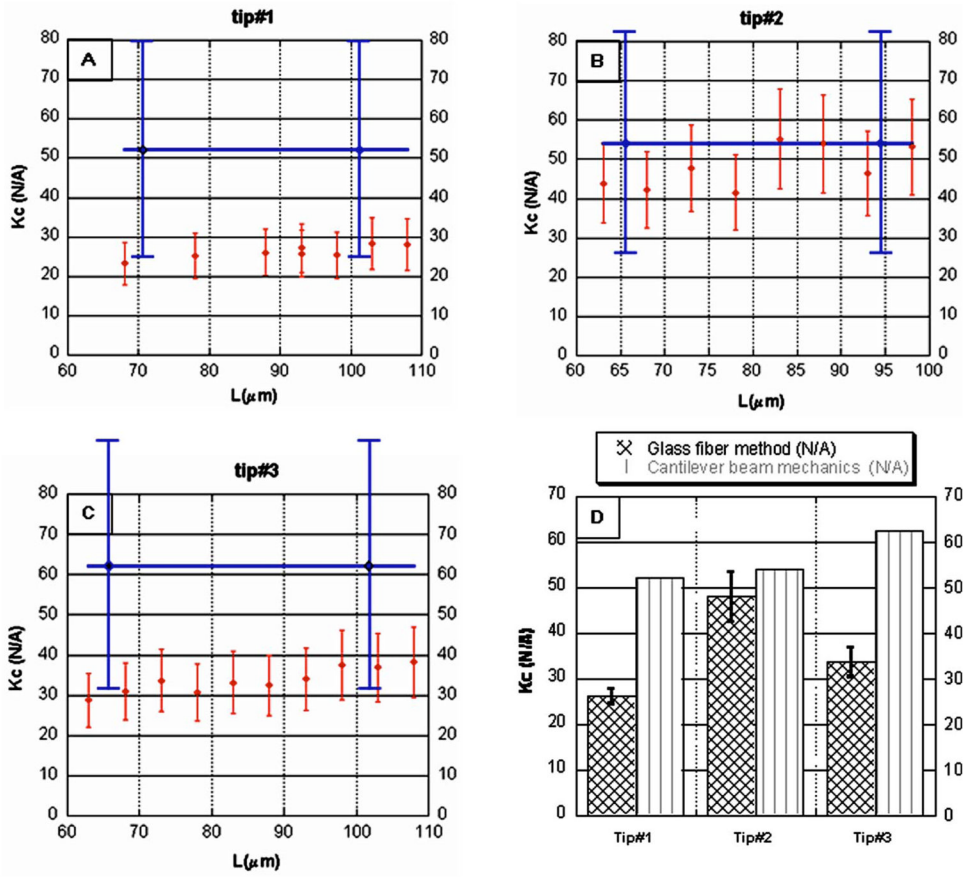

FIG. 5.

(Color online) [(A–C)] The lateral force conversion factor K_C plotted vs length of the glass fiber (touching point) for each of the three tips. The red diamonds show the results as obtained from glass fiber bending experiments like in Fig. 4. Each tip made at least eight pushes at various lengths of the glass fiber L. The error bars correspond to the uncertainty of 26% for this method (see text). The straight, blue line corresponds to K_C as calculated from dimensions of the cantilevers and the sensor response [theoretical method, Eq. (10)]. The error bar corresponds to an uncertainty of 56% for this method (see text). (D) K_C averaged over all L values for each tip. Here, the error bars correspond to the standard deviation of the measurements for each tip.

NIH-PA Author Manuscript NIH-PA Author Manuscript NIH-PA Author Manuscript

TABLE I

Cantilever properties as determined from beam mechanics. The table lists the dimensions, resonance frequency, and force constants of the three cantilevers used in these experiments. The length L, the width w, and the tip height h were measured via optical microscopy; the resonance frequency, f_0, was obtained from the standard AFM resonance curve, and it was used to determine the thickness via Eq. (4b); the normal and lateral spring constants, k_n and k_l, were determined via beam mechanics [Eqs. (2) and (6)]. K_C was determined through cantilever beam mechanics via Eq. (10) (second to last column) and the glass fiber method (last column). The errors are 56% and 26%, respectively (see text).

Tip no.	L (μm)	h (μm)	w (μm)	t (μm)	f_0 (kHz)	k_n (N/m)	k_l (N/m)	K_C (N/A)	K_C (N/A)
1	348	22.3	41.7	1.08	9.328	0.053	4.83	52.2±29.2	26.2±6.0
2	286	16.7	40.8	1.70	25.8	0.361	37.8	54.1±30.3	48.0±11.0
3	249	22.2	42.1	2.28	42.02	1.38	62.1	62.3±34.9	33.6±7.7

Rev Sci Instrum. Author manuscript; available in PMC 2011 January 11.